Semi-parametric estimation without searching in function space.

Application to *in vivo* metabolite quantitation

E. Popa[1], D.A. Karras[2], B.G. Mertzios[3], D. Sima[4], R. de Beer[5], D. van Ormondt[5], D. Graveron-Demilly[1]

[1]Laboratoire CREATIS-LRMN; CNRS UMR 5220; INSERM U630; Université Claude Bernard Lyon 1, FR; [2]Chalkis Institute of Technology, Dept. Automation, GR; [3]Democritus University of Thrace, GR; [4]Dept. Electrical Engineering (ESAT), Katholieke Universiteit Leuven, BE; [5]Applied Physics, Delft University of Technology, NL

E-mail: `d.vanormondt@tudelft.nl, danielle.graveron@univ-lyon1.fr`

Abstract. Magnetic Resonance Spectroscopy (MRS) is the method of choice for noninvasive *in vivo* measurement of metabolites in patients. When the model function describing the acquired MRS signal is incomplete, semi-parametric techniques are required for estimation of the wanted metabolite concentrations. In the present work, incompleteness means that the model function of the MRS signal-decay is unknown. We devised the simplest method yet for avoiding cumbersome searches in function space, attendant on semi-parametric estimation. This is based on the assumption that all sinusoids in the MRS signal have equal decay and that this decay has no high-frequency components. Application of the method through a plug-in for the metabolite quantitation software package jMRUI is envisaged.

PACS numbers: 87-61.-c, 87.85.Ng

Keywords: Semi-parametric estimation, parameter space, function space, hyper-parameters, MR spectroscopy, *in vivo*, unknown lineshape

Submitted to: *Meas. Sci. Technol.*

1. Introduction

Noninvasive *in vivo* measurement of metabolites in a patient is best achieved with Magnetic Resonance Spectroscopy (MRS); see, *e.g.*, [1–3]. Usually, estimation of the metabolite concentrations is done by fitting an appropriate physical model function to the acquired MRS signal by a search in the corresponding physical parameter space [4]. The notion of 'physical' is used to distinguish model functions describing physical phenomena, such as magnetic resonance, from 'mathematical' functions such as, *e.g.*, Fourier expansions. This distinction is made because the MRS model function may be incomplete, *i.e.*, the acquired signal can only be partially described by a physical function. The nondescript part of the signal in question must be handled by a search in so-called *function* space [5] which is a mathematical rather than a physical contraption. When a model function is partly physical and partly mathematical, one speaks of semi-parametric estimation [6]. A search in function space is rather more cumbersome than a search in parameter space. Consequences are that the theory of Cramér-Rao Bounds (CRB) on estimation errors ceases to hold and that bias is incurred; see, *e.g.*, [7–9].

This manuscript reports on further development of our new estimation method which, although semi-parametric, circumvents a search in function space. Only a search in the physical model parameter space is needed. To this end, we invoke general, non-critical, *a priori* knowledge. One advantage of this approach is that the notion of inadvertently excluding some essential part of function space does not exist, thus reducing the risk of incurring bias. No user interaction is needed to attain an accuracy as high as 10 decimal positions, with a noiseless signal.

The method was tested on simulated signals so as to be able to correctly judge accuracy and precision of the semi-parametric estimates. A plug-in version, to be included in the metabolite quantitation package jMRUI [10], is submitted to this Issue of MST too. The latter work includes a realistically mimicked *in vivo* MRS signal.

In the sequel, we treat our MRS metabolite model function and restrictions imposed on it derived from *a priori* knowledge so as to avoid the search in function space normally needed in semi-parametric estimation. Next, we treat the principle of the method, and subsequently two variations with different merits related to noise in the signal.

2. Methods

2.1. The MRS Model Function of Metabolites

In vivo MRS is done on MRI-scanners with extra facilities for spectroscopy [11]. An MRS signal is a complex-valued pulse-response acquired in the time-domain. Depending on the ambient physical conditions, a metabolite signal decays into the noise within a period of several ms to 1 s. Recall that the Fourier Transform (FT) of the decay corresponds

to the functional form of spectral lines (lineshapes) in the frequency-domain.
The main aspect of this work is how to estimate metabolite concentrations in the case that the functional form of the decay is *a priori* unknown. We assume that a so-called reference signal from which the functional form of the decay can be estimated is not available.
As an introduction, we treat first the relatively simple case of metabolites in liquid solution, *in vitro*, where the functional form of the decay is known. Subsequently, we treat the rather more complicated case of metabolites in humans, *in vivo*, at high applied magnetic field B_0, where the functional form of the decay is often unknown.

2.1.1. Metabolites in liquid solution. Parametric estimation

The model function of a signal obtained from $m = 1, \ldots, M$ different metabolite species can be written as

$$\hat{s}(t) = \sum_{m=1}^{M} c_m \, \hat{s}_m(t) \quad , \tag{1}$$

where $t = n\triangle t$ is the real time, $\triangle t$ is the sample interval, $\hat{s}_m(t)$ is the model function of metabolite species $\#m$, c_m the corresponding concentration. A 'hat' on a symbol denotes that one deals with a model function, without specifying whether that model function is analytical or numerical. The model function of metabolite species $\#m$, in turn, can be written as

$$\hat{s}_m(t) = \sum_{k=1}^{K_m} a_k^m \, d_k^m(t) \, e^{\imath \, 2\pi \nu_k^m t + \imath \, \varphi_k^m} \quad , \tag{2}$$

where a_k^m, $d_k^m(t)$, ν_k^m, φ_k^m are the amplitude, decay, frequency, phase, respectively of the $k = 1, \ldots, K_m$ sinusoids of metabolite species $\#m$; $\imath = \sqrt{(-1)}$. Depending on the chemical composition of metabolite species $\#m$, K_m can be $1, \ldots, > 10$. When metabolites are dissolved in some liquid, *in vitro*, the functional form of the decay is approximately exponential [12], *i.e.*,

$$\hat{d}_k^m(t) \approx e^{\alpha_k^m t}, \qquad \alpha_k^m < 0 \quad . \tag{3}$$

The model function resulting from combination of Eqs. 1, 2, 3 can be handled by conventional parametric estimation. If no *a priori* knowledge of model parameters is used, one needs to estimate $c_m, K_m, a_k^m, \alpha_k^m, \nu_k^m, \varphi_k^m$ for all m and k. The number of parameters can be as high as one hundred, but since decay is slow in liquid solutions, thousands of signal samples are usually available. As a rule, the decay constants α_k^m will be found to depend on m and k.

2.1.2. Metabolites in vivo. Semi-parametric estimation

The decay of metabolite signals of humans, *i.e. in vivo*, is often very different. This has to do with macro- and micro-scale heterogeneity within a human (or animal, for that matter) body: Its multiple tissue types and regions filled with fluid or air all have different magnetic susceptibilities, causing *inhomogeneity* of the applied magnetic

field B_0 in a region of interest. Since the frequencies of the sinusoids contained in the signal are proportional to B_0, inhomogeneity of B_0 affects the shapes of spectral lines. This, in turn, affects the functional form of the decay, in an *a priori* unknown way. It has been demonstrated that at high B_0, the contribution of inhomogeneity to the decay can *dominate* that of all other mechanisms, see *e.g.* [13–17]. Assuming then that decay mechanisms other than B_0 inhomogeneity are insignificant, and that the spatial distributions of the metabolites, see *e.g.* [18], are equal, the decays of all individual sinusoids making up the signal should be approximately equal. We shall refer to this condition as 'common decay'. It constitutes powerful *a priori* knowledge for semi-parametric estimation. At the same time, we emphasise that the functional form of the common decay is *a priori* unknown because it is caused by *a priori* unknown heterogeneity of the human body. However, by viewing the spectrum FT$[s(t)]$ one can easily verify that width of individual features is usually much smaller than the width of the total spectral region displayed. This enables one to impose an upper frequency threshold, $\nu_{\text{threshold}}$, on any features contained in FT$[d(t)]$. The value of $\nu_{\text{threshold}}$ appeared not critical.

In the remainder of this subsection, we make up for the loss of information caused by B_0-inhomogeneity by simulating a metabolite signal database and by mathematical exploitation of common decay.

– *Database of non-decaying metabolite signals,* $s_m^{\text{nodecay}}(t)$
Inhomogeneity of B_0 broadens the spectral lines considerably. As a consequence, *in vivo* measurement of the complete set of parameters $K_m, a_k^m, \nu_k^m, \varphi_k^m, k = 1, \ldots, K_m$, $m = 1, \ldots, M$, is not possible. Fortunately, progress in computational physics enables their quantum-mechanical calculation, see *e.g.* [10], using specific molecular properties, see *e.g.* [19], of each metabolite species. Treating the resulting parameters as constants, one can simulate a database of non-decaying, numerical metabolite model functions, $s_m^{\text{nodecay}}(t)$, written as

$$s_m^{\text{nodecay}}(t) = \sum_{k=1}^{K_m} a_m \, e^{\imath\, 2\pi \nu_k^m t + \imath\, \varphi_k^m} \quad , \; m = 1, \ldots, M. \tag{4}$$

In the subsequent semi-parametric estimation process, the metabolite signal database is *fixed*; therefore, no hat is placed on $s_m^{\text{nodecay}}(t)$. However, 'last-minute' tuning of various frequencies ν_k^m to the signal at hand is possible [20]. In addition, one can shift all $\nu_k^m, k = 1, \ldots, K_m$ by the same small amount, $\triangle\nu_m$, for each m, and add the set $\triangle\nu_m, m = 1, \ldots, M$ to $c_m, m = 1, \ldots, M$, to be estimated from the *in vivo* signal.

Table 1 shows the parameter values of the non-decaying, fictitious metabolite signal database used in this work. Three metabolites are used, *i.e.*, $M = 3$. The signals for $m = 1, 2$ each contain four sinusoids. Their frequencies ν_k^m have been chosen such that the corresponding spectra in the frequency-domain overlap considerably, corresponding

Table 1. The parameters of the non-decaying[§] part of the simulated, fictitious metabolite signal $s(t)$ and the non-decaying signals of the database $s_m^{\text{nodecay}}(t), m = 1, 2, 3$, with $t = n\triangle t, n = 1, \ldots N$, of Eq. (4).

m	k	a_k^m	$\nu_k^{m\dagger}$	$\varphi_k^{m\ddagger}$
1	1	0.50	0.150	0.0
	2	1.50	0.160	60.0
	3	1.50	0.170	120.0
	4	0.50	0.180	180.0
2	1	0.30	0.130	0.0
	2	0.60	0.150	30.0
	3	0.90	0.170	60.0
	4	1.20	0.190	90.0
3	1	1.00	-0.160	0.0

† Frequencies are in units of $1/(\triangle t)$, *i.e.*, $-0.5 \leq \nu < 0.5$.

‡ In units of degrees.. § See [21] for details about $d(t)$.

to complicated real-world conditions. The signal for $m = 3$ consists of only one sinusoid.

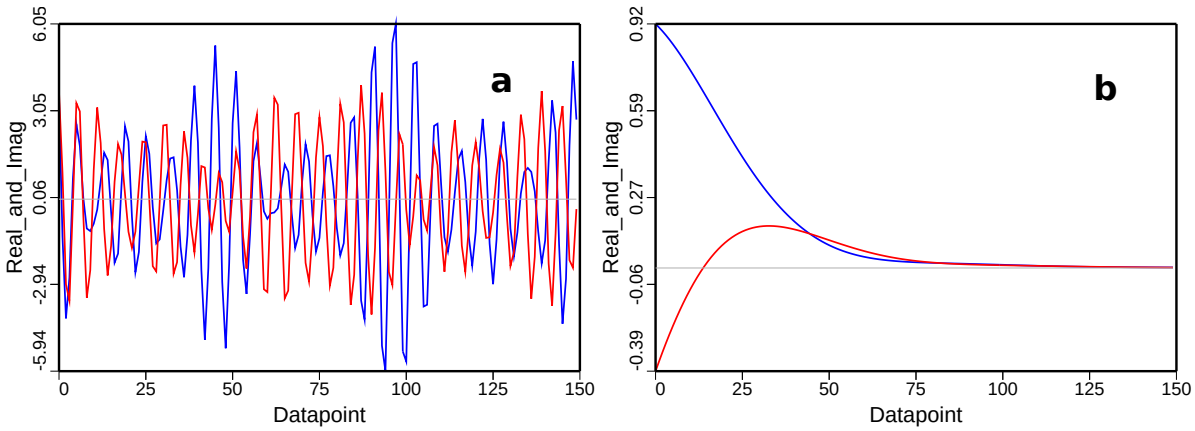


Figure 1. **a**: Plot of $s^{\text{nodecay}}(t) = \sum_{m=1}^{3} c_m\, s_m^{\text{nodecay}}(t), \quad c_1 = 0.5, c_2 = 1.0, c_3 = 2.0.$ **b**: Plot of simulated $d(t)$; see [21] for details. Blue: Real part. Red: Imaginary part. The simulated signal (data) equals the product of the two: $s(t) = d(t)\, s^{\text{nodecay}}(t)$.

– *Simulation of the metabolite signal, $s(t)$*

The simulated signal, $s(t)$, representing some difficult metabolite signal which comprises heavily overlapping (frequency-wise) components, was constructed from the database mentioned above, using $c_1 = 0.5, c_2 = 1.0, c_3 = 2.0$. Fig. 1a shows the non-decaying version of $s(t)$. This was multiplied with the decay function shown in Fig. 1b; see [21] for details. Its functional form was deliberately chosen so as to deviate considerably from

exponential decay. In fact, its spectral shape in the frequency-domain is asymmetric. In actual *in vivo* MRS practice, the width of the spectral shape, FT$[d(t)]$, is limited to only a few percent of the full spectral width $1/(\triangle t)$. (FT stands for Fast Fourier Transform.) The entity $\nu_{\text{threshold}}$, introduced above, relates to this. Together with common decay it constitutes powerful prior knowledge that forms the basis of our method.

– *Exploitation of common decay*

The phenomenon of 'common decay' is now exploited by dropping the subscripts k and superscript m, *i.e.*,

$$d_k^m(t) \rightarrow d(t), \quad k = 1, \ldots, K_m, \quad m = 1, \ldots, M, \tag{5}$$

enabling us to take the unknown decay out of the summation in the model function $\hat{s}(t)$, leading to the simple expression

$$\hat{s}(t) = d(t) \sum_{m=1}^{M} c_m \, e^{\imath \, 2\pi \triangle \nu_m t} \, s_m^{\text{nodecay}}(t). \tag{6}$$

Eq. (6), however simple, represents the typical formidable semi-parametric case. The magnitude of the problem pertains to the fact that the functional form of the decay is unknown. Although decay carries no useful biomedical information, its (partial) estimation can not be avoided. As a first step in this process, we generate starting values of $c_m, \triangle\nu_m, m = 1, \ldots, M$ by substituting exponential decay into Eq. (6) and fitting the resulting $\hat{s}(t)$ to the signal $s(t)$, yielding

$$\tilde{d}(t) \approx \frac{s(t)}{\sum_{m=1}^{M} c_m \, e^{\imath \, 2\pi \triangle \nu_m t} \, s_m^{\text{nodecay}}(t)} \quad , \tag{7}$$

where $c_m, \triangle\nu_m, m = 1, \ldots, M$ have been given the starting values mentioned above. The tilde indicates a numerical representation.

Merely replacing $d(t)$ of Eq. (6) by $\tilde{d}(t)$ of Eq. (7) does not yield new results [21]. Yet, normalisation of $\tilde{d}(t)$ according to $\tilde{d}(t = 0) = 1$, does improve metabolite quantitation obtained with an incorrect function like exponential decay [21].

– *Modelling of* $\tilde{d}(t)$

The proper continuation after arriving at Eq. (7) is to *model* $\tilde{d}(t)$, using tools like HSVD [22, 23], Splines [24], Wavelets [24], or Lowess [25], and to then substitute the result into Eq. (6). Fitting the resulting $\hat{s}(t)$ to the signal $s(t)$ with Non-Linear Least Squares (NLLS), usually yields much better estimates of $c_m, \triangle\nu_m, m = 1, \ldots, M$. A few iterations of this procedure can improve the estimates even further.

Modelling of a numerical function like $\tilde{d}(t)$ is usually referred to as 'non-parametric estimation' because the many parameters involved pertain to a mathematical rather than a physical model function. In fact, such modelling amounts to a *'search in function space'*; see, *e.g.*, [5], page 309. The number of mathematical model parameters required to obtain a good fit is referred to as *hyper-parameter*. Optimising hyper-parameters may

not be an easy task.
The next subsection shows how a search in function space can be avoided. The advantage is that, apart from the physical parameters $c_m, \triangle\nu_m, m = 1, \ldots, M$, no new parameters need be introduced.

2.2. Avoiding the Search in Function Space of Semi-parametric Estimation

Since searching in function space involves estimation of many physically irrelevant parameters, trying to avoid it is worthwhile. Our present method, evolved from [21], is described below. In order to simplify its explanation, the noiseless case is treated first.

2.2.1. Noiseless case

A noiseless signal can be expressed as

$$s^{\text{noiseless}}(t) = d(t)^{\text{true}} \sum_{m=1}^{M} c_m^{\text{true}}\ e^{\imath 2\pi \triangle\nu_m^{\text{true}}\, t}\ s_m^{\text{nodecay_true}}(t) \quad , \tag{8}$$

where the superscript 'true' indicates that the entity in question has the true, experimental value. Comparing then Eq. (8) with the model function Eq. (6), and assuming that the database signals are accurate, it follows that $\tilde{d}(t)$ becomes accurate once the $c_m, \triangle\nu_m, m = 1, \ldots, M$ approach the true values. Inaccuracy of the parameters is manifested as appearance of high-frequency components in $\tilde{d}(t)$ [21–25]. According to *a priori* knowledge about the spectral width of FT$[d(t)]$ mentioned above, such high-frequency components should not occur. In this example, $\nu_{\text{threshold}} = 0.15$, to be compared with the full spectral range of $\nu_{\text{min}} = -0.5$, $\nu_{\text{max}} = 0.5$. This value is not critical. The gist of the method is that high-frequency components can be removed *directly by adjusting the values of* $c_m, \triangle\nu_m, m = 1, \ldots, M$, instead of by modelling $\tilde{d}(t)$ in function space. The values resulting in removal are the wanted ones.

Fig. 2 provides a flowchart of this direct estimation of the wanted metabolite parameters for the simulated signal described above. In essence, the method is as follows. First, components with $|\nu| < \nu_{\text{threshold}}$ are stripped from $\tilde{d}(t)$ with a high-pass filter. Next, the remaining components, with $|\nu| > \nu_{\text{threshold}}$, are reduced to zero by a Non-Linear Least-Squares (NLLS) procedure involving the physical model parameters c_m, $\triangle\nu_m, m = 1, \ldots, M$ only. In absence of noise, correct values of the concentrations c_1, c_2, c_3 of the case at hand [21] can be obtained up to about ten decimal positions.

Before proceeding to the noisy case, we establish the following points.

- As for the values of $c_m, m = 1, 2, \ldots, M$, correctness of their ratios suffices to suppress the high-frequency components in $\tilde{d}(t)$. Multiplying each c_m with the same number will result in mere division of $\tilde{d}(t)$ by that number.
- The values of $c_m, m = 1, 2, \ldots, M$ become absolute ‡ by adjusting them such that $\tilde{d}(0) = s(0)/\hat{s}(0)^{\text{nodecay}} = 1$.

‡ Here 'absolute' is in the context of absolute versus relative, not in the context of positive and negative.

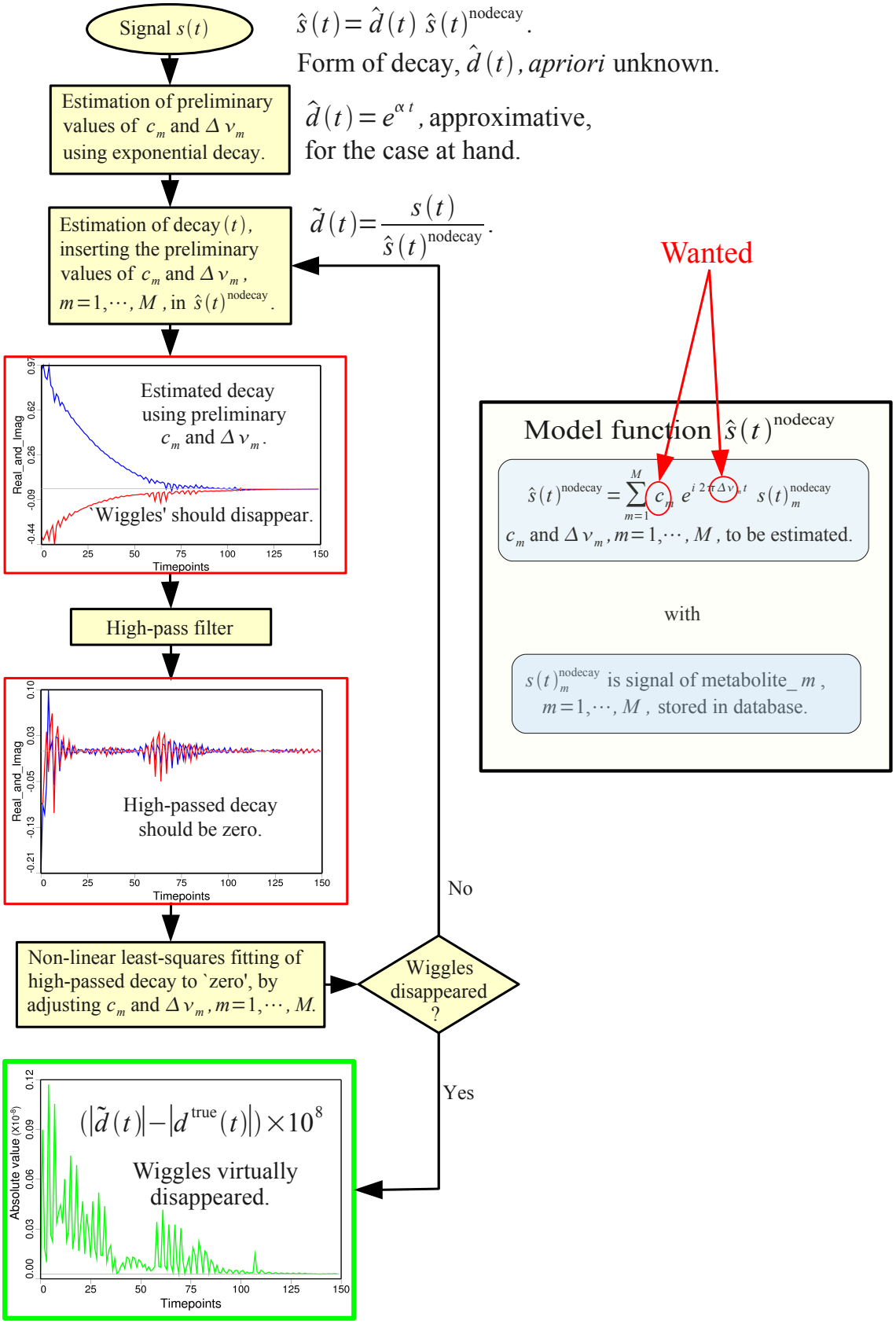


Figure 2. Flowchart of direct estimation of the wanted metabolite parameters $c_m, \triangle\nu_m, m = 1, 2, \ldots, M$. The displayed plots pertain to the noiseless case. 'Wiggles' stands for high-frequency components. $\nu_{\text{threshold}} = 0.15$, to be compared with the full spectral range of ± 0.5. See text.

- Anticipating on the noisy case, Sec. 2.2.2, the previous point implies that the noise in only $s(0)$ determines the error in the absolute values. The error in relative values (ratios) is determined solely by the process depicted in Fig. 2.

2.2.2. Noisy case

Using Eq.(8), we write

$$s(t) = s^{\text{noiseless}}(t) + \text{noise}(t) \ , \tag{9}$$

in which noise(t) stands for noise in the signal. It follows then from Eq. (7) that noise(t) in $s(t)$ becomes modulated noise in $\tilde{d}(t)$ through multiplication by $\left(\tilde{s}(t)^{\text{nodecay}}\right)^{-1} = \left(\sum_{m=1}^{M} c_m \ e^{\imath\, 2\pi \triangle\nu_m t} \ s_m^{\text{nodecay}}(t)\right)^{-1}$:

$$\tilde{d}(t) \approx \frac{s^{\text{noiseless}}(t) \ + \ \text{noise}(t)}{\sum_{m=1}^{M} c_m \ e^{\imath\, 2\pi \triangle\nu_m t} \ s_m^{\text{nodecay}}(t)} \quad , \tag{10}$$

Fig. 3 shows that the modulation makes noise(t) spiky. The spikes, in turn, perturb the high-frequency components (wiggles in Fig. 2) and thereby hamper the NLLS-procedure aimed at removing wiggles. Nevertheless, the approach is still beneficial at the usual level of measurement noise [21]. Two reasons for this can be given.

(i) The NLLS-criterion shown in Fig. 2 can be made to work in tandem with the traditional criterion of minimising $|s(t) - \hat{s}(t)|^2$ [21]. This alleviates the effect of noise spikes.

(ii) The NLLS-criterion shown in Fig. 2 can be transformed to the frequency domain by FT. FT of modulated noise amounts to convolution of FT[noise] and FT[modulation]. Fig. 3f shows that the convolution 'scrambles' noise spikes visible in Fig. 3e. This may explain our finding that, so far, root-mean-square errors in the metabolite concentrations are consistently up to about 10% lower when the high-frequency components in $\tilde{d}(t)$ are removed in the frequency domain.

3. Discussion

3.1. Semi-parametric Estimation

Semi-parametric estimation is a vast subject still under development. This applies especially to *in vivo* MRS where new measurement techniques appear continually. Hence, our contribution is to be considered a work in progress. Below, we discuss the following aspects.

Main result The main result is that we devised semi-parametric estimation of physical parameters in its simplest form yet; see Fig, 2. Contrary to the version proposed in [21], the new version takes place entirely in the measurement-domain (time-domain) for the first time. The green box at the bottom of Fig, 2 shows the residue $(|\tilde{d}(t)| - |d^{\text{true}}(t)|) \times 10^8$ for the noiseless, simulated metabolite signal, shown in

Fig. 1a, multiplied by the decay shown in Fig. 1b. Note that the method is not aimed at estimating the full decay, but primarily at removing its components with

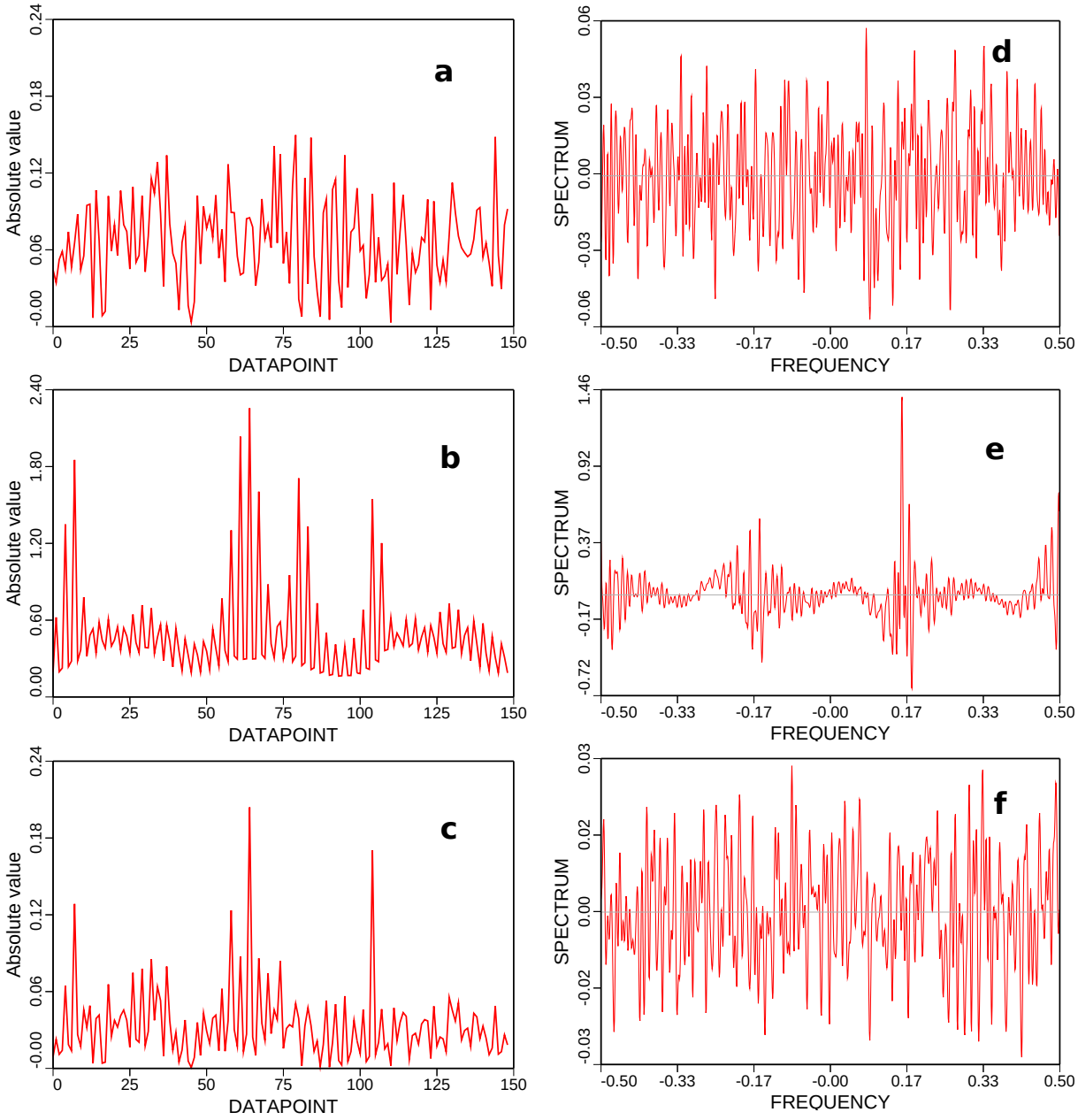


Figure 3. Modulation of noise(t) by the function $\left(\tilde{s}(t)^{\text{nodecay}}\right)^{-1}$, in two domains.
Left: Multiplication in the time-domain.
a. noise(t). **b**. $\left(\tilde{s}(t)^{\text{nodecay}}\right)^{-1}$. **c**. Modulated noise: noise(t) $\left(\tilde{s}(t)^{\text{nodecay}}\right)^{-1}$, giving rise to spikes that can hamper the Non-Linear Least-Squares (NLLS) procedure mentioned in Sec. 2.2.2 and Fig. 2.
Right: Convolution in the frequency-domain. Note the differences in vertical scale.
d. Re FT [noise(t)] in $s(t)$. **e**. Re FT $[\left(\tilde{s}(t)^{\text{nodecay}}\right)^{-1}]$.
f. Re FT [noise(t) $\left(\tilde{s}(t)^{\text{nodecay}}\right)^{-1}$], amounting to *convolution* of the spectra in **d,e**. No spikes arise. FT stands for Fourier Transform.

$|\nu| > \nu_{\text{threshold}}$, by adjusting the parameters c_m, $\triangle\nu_m, m = 1, \ldots, M$ only.

Application The method is presently being tested for real-world *in vivo* MRS signals and simulations mimicking these signals as closely as possible. The latter research is taking place in the context of enhancing the metabolite quantitation software package jMRUI [10]. Among other things, it involves adding the new method to the jMRUI as plug-in. The variant that partly uses the frequency-domain for reducing sensitivity to noise, see Fig. 3d,e,f, was chosen. Designing and testing the plug-in being a subject in itself requiring working knowledge of Java, this work is submitted separately to same Issue of MST (de Beer, *et al* .).

Spurious signals So far, our method is restricted to signals with contributions from metabolites only. However, this is not a limitation because it will be plugged into the metabolite quantitation software package jMRUI, as mentioned above. The jMRUI enables removal of spurious signals from macromolecules, water, and lipids, and includes exponential decay in its NLLS fit procedure. Depending on the need, the metabolite concentrations estimated by jMRUI can subsequently be improved with the new plug-in. In addition, we mention recent substantial progress in suppression of the signal from macromolecules by a new scan technique [26], resulting in a cleaner signal.

NLLS-procedure Fig. 3 shows that the noise in $\tilde{d}(t)$ is far from Gaussian. As a result, using an NLLS-procedure as indicated in Fig. 2 can not be optimal [4]. Possibly, algorithms that are more robust in the presence of outliers, such as [27, 28], are preferable.

Cramér-Rao Bounds In semi-parametric estimation, the model function is partly unknown, by definition. As a consequence, the theory of Cramér-Rao Bounds (CRB) is invalid; see, *e.g.*, [7]. In the parametric case, a favourable aspect of CRBs is their independence of the estimator used, which is very useful for experimental design. In the semi-parametric case, estimation errors depend on how one conducts the search in function space; infinite variations are possible. So far, our new method has not brought solace in this matter.

Analytical decay function Starting values for $\tilde{d}(t)$ were obtained by initially setting $\hat{d}(t) = e^{\alpha t}$. If the signal-to-noise ratio (SNR) of a metabolite signal is low, bias due to inadequacy of exponential decay may be less than the standard deviation due to noise. Application of the present method may then not outweigh the attendant effort. In fact, automated judgement of possible adequacy of an approximative analytic version of $\hat{d}(t)$ at a given SNR is desirable. This facility is presently not available.

3.2. Justification of Common Decay

As mentioned in Sec. 2.1.2, inhomogeneity of B_0 constitutes the dominant contribution to the decay of metabolite signals from the brain at very high B_0. When minimising macro-scale inhomogeneity of B_0 by so-called shimming [29] is successful, micro-scale

inhomogeneity of B_0 becomes the next dominant contributor [30]. It seems that not only macro-susceptibility effects but also micro-susceptibility effects give rise to common decay in the brain. The spatial distribution of metabolites, see *e.g.* [18, 31, 32], supposedly plays a role in these matters. Finally, note that research on higher-order (> 2) shimming is ongoing [33, 34]. The need for this is apparent from cases like [13–17].

4. Conclusions

- We devised a simple form of semi-parametric estimation that avoids the usual search in function space. Its simplest form yet is explained in detail.
- The underlying *a priori* knowledge is
  - The decays of all sinusoids in the signal are equal (common decay).
  - The common decay lacks high-frequency components.
- The method will become available as plug-in of the metabolite quantitation software package jMRUI.

Acknowledgment

Supported by Marie Curie Research Training Network 'FAST' (MRTNCT -2006-035801, 2006-2010).

References

[1] C.E. Mountford, P. Stanwell, A. Lin, S. Ramadan, and B. Ross. Neurospectroscopy: The Past, Present and Future. *Chem. Rev.*, 110:3060–3086, 2010. 2

[2] K. Glunde, D. Artemov, M.-F. Penet, M.A. Jacobs, and Z.M. Bhujwalla. Magnetic Resonance Spectroscopy in Metabolic and Molecular Imaging and Diagnosis of Cancer. *Chem. Rev.*, 110:3043–3059, 2010.

[3] W. Bogner, S. Gruber, M. Doelken, A. Stadlbauer, O. Ganslandt, U. Boettcher, S. Trattnig, A. Doerflerand, H. Stefane, and T. Hammen. In vivo quantification of intracerebral GABA by single-voxel ^{1}H-MRS — How reproducible are the results? *European Journal of Radiology*, 73:526–531, 2010. 2

[4] A. van den Bos. *Parameter Estimation for Scientists and Engineers*. Wiley, 2007. 2, 11

[5] C.H. Kim, A.R. Mijar, and J.S. Arora. Development of simplified models for design and optimization of automotive structures for crashworthiness. *Struct Multidisc Optim*, 22:307–321, 2001. 2, 6

[6] P.J. Bickel, C.A.J. Klaassen, Y. Ritov, and J.A. Wellner. *Efficient and Adaptive Estimation for Semiparametric Models*. Springer, paperback 1998. 2

[7] H. Ratiney, Y. Coenradie, S. Cavassila, D. van Ormondt, and D. Graveron-Demilly. Time-Domain Quantitation of ^{1}H Short Echo-Time Signals: Background Accommodation. *Magnetic Resonance Materials in Physics Biology and Medicine*, 16(6):284–296, May 2004. 2, 11

[8] H. Ratiney, M. Sdika, Y. Coenradie, S. Cavassila, D. van Ormondt, and D. Graveron-Demilly. Time-Domain Semi-Parametric Estimation Based on a Metabolite Basis Set. *NMR in Biomedecine*, 18:1–13, 2005.

[9] J.B. Poullet, D.M. Sima, and S. Van Huffel. MRS signal quantitation: A review of time- and frequency-domain methods. *Journal of Magnetic Resonance*, 195(2): 134–144, 2008. 2

[10] D. Stefan, F. Di Cesare, A. Andrasescu, E. Popa, A. Lazariev, E. Vescovo, O. Strbak, S. Williams, Z. Starcuk, M. Cabanas, D. van Ormondt, and D. Graveron-Demilly. Quantitation of magnetic resonance spectroscopy signals: the jMRUI software package. *Meas. Sci. Technol.*, 20:104035 (9pp), 2009. 2, 4, 11

[11] R.A. de Graaf. *In Vivo NMR Spectroscopy: Principles and Techniques*. Wiley, 2nd edition, 2007. 2

[12] A. Abragam. *The principles of nuclear magnetism*. Oxford at the Clarendon Press, 1961. 3

[13] O. Gonen, S. Gruber, B.S.Y. Li, V. Mlynarik, and E. Moser. Multivoxel 3D Proton Spectroscopy in the Brain at 1.5 Versus 3.0 T: Signal-to-Noise Ratio and Resolution Comparison. *Am J Neuroradiol*, 22:1727–1731, 2001. 4, 12

[14] G.V. Shah, D. Gandhi, and S.K. Mukherji. Magnetic Resonance Spectroscopy of Head and Neck Neoplasms. *Topics in Magnetic Resonance Imaging*, 15:87–94, 2004.

[15] C. Juchem, N.K. Logothetis, and J. Pfeuffer. ^{1}H-MRS of the macaque monkey primary visual cortex at 7 T: strategies and pitfalls of shimming at the brain surface. *Magnetic Resonance Imaging*, 25(6):902–912, 2007.

[16] C. Choi, I.E. Dimitrov, D. Douglas, A. Patel, L.G. Kaiser, C.A. Amezcua, and E.A. Maher. Improvement of resolution for brain coupled metabolites by optimized 1H MRS at 7 T. *NMR in Biomedicine*, 23:1044–1052, 2010.

[17] S. Li, Y. Zhang, S. Wang, M. Ferraris Araneta, C.S. Johnson, Y. Xiang, R.B. Innis, and J. Shen. ^{13}C MRS of occipital and frontal lobes at 3 T using a volume coil for stochastic proton decoupling. *NMR in Biomedicine*, 23:977–985, 2010. 4, 12

[18] S-T. Hong, D.Z. Balla, G. Shajan, C. Choi, and R. Pohmann. Regional Variations of Metabolite Concentrations in the Rat Brain Assessed with in vivo ^{1}H MR Spectroscopy at 16.4T. In *Proc. ISMRM*, Stockholm, SE, 1–7 May 2010. 4, 12

[19] Z. Atieh, A.R. Allouche, D. Graveron-Demilly, F. Fauvelle, and M. Aubert-Frécon. Density functional theory calculations of the nuclear magnetic resonance spin-Hamiltonian parameters for two polyamines of prostate tissue: spermidine and spermine. *Meas. Sci. Technol.*, 20:104024, 2009. 4

[20] A. Lazariev, A-R. Allouche, M. Aubert-Frécon, F. Fauvelle, K. Elbayed, M. Piotto, I.J. Namer, D. van Ormondt, and D. Graveron-Demilly. Optimization of metabolite basis-sets prior to quantitation: a Quantum Mechanics approach. In *IEEE International Workshop on Imaging Systems and Techniques, IST 2010*, pages 365–368, Thessaloniki, GR, 1–2 July 2010. 4

[21] E. Popa, E. Capobianco, R. de Beer, D. van Ormondt, and D. Graveron-Demilly. In vivo quantitation of metabolites with an incomplete model function. *Meas. Sci. Technol.*, 20:104032 (9pp), 2009. 5, 6, 7, 9

[22] H. Rabeson, E. Capobianco, R. de Beer, D. van Ormondt, and D. Graveron-Demilly. Correction pour l'inhomogénéité de B_0 et effets de courant de Foucault sans utiliser un signal de référence. In *Book of Abstracts*, page 101, 12ème Congrès du GRAMM, Lyon, FR, 26-28 March 2008. Groupe de Recherche sur les Applications du Magnétisme en Médecine, http://gramm.ujf-grenoble.fr/. 6

[23] E. Popa, E. Capobianco, R. de Beer, D. van Ormondt, and D. Graveron-Demilly. Improved lineshape estimation in absence of a reference peak. In *Book of Abstracts*, page 75, Antwerp, BE, 10 December 2008. First Annual Meeting of the Benelux ISMRM Chapter. 6

[24] D.M. Sima, M.I. Osorio Garcia, J-B. Poullet, A. Suvichakorn, J-P. Antoine, S Van Huffel, and D. van Ormondt. Lineshape estimation for magnetic resonance spectroscopy (MRS) signals: self-deconvolution revisited. *Meas. Sci. Technol.*, 20: 104031 (12pp), 2009. 6

[25] E. Popa. *Algorithms for Handling Arbitrary Lineshape Distortions in Magnetic Resonance Spectroscopy and Spectroscopic Imaging*. PhD thesis, Université Claude Bernard – Lyon 1, 2010. 6, 7

[26] N. Kunz, C. Cudalbu, V. Mlynarik, P.S. Huppi, S.V. Sizonenko, and R. Gruetter. Diffusion-Weighted Spectroscopy: A Novel Approach to Determine Macromolecule Resonances in Short-Echo Time ^{1}H-MRS. *Magnetic Resonance in Medicine*, 64: 939–946, 2010. 11

[27] P.J. Rousseeuw. Least Median of Squares Regression. *Journal of the American Statistical Association*, 79:871–880, 1984. 11

[28] Y. Li and G.R. Arce. A Maximum Likelihood Approach to Least Absolute Deviation Regression. *EURASIP Journal on Applied Signal Processing*, 12:1762–1769, 2004. 11

[29] R. Gruetter. Automatic, Localized *in Vivo* Adjustment of All First- and Second-Order Shim Coils. *Magnetic Resonance in Medicine*, 29:804–811, 1993. 11

[30] D.K. Deelchand, P-F. Van de Moortele, G. Adriany, I. Iltis, P. Andersen, J.P. Strupp, J.P. Vaughan, K. Uğurbil, and P-G. Henry. *In vivo* ^{1}H NMR spectroscopy of the human brain at 9.4 T: Initial results. *Journal of Magnetic Resonance*, 206: 74–80, 2010. 12

[31] J. Pfeuffer, I. Tkac, and R. Gruetter. Extracellular-Intracellular Distribution of Glucose and Lactate in the Rat Brain Assessed Noninvasively by Diffusion-Weighted ^{1}H Nuclear Magnetic Resonance Spectroscopy *In Vivo*. *Journal of Cerebral Blood Flow & Metabolism*, 20:736–746, 2000. 12

[32] S-C. Lee, J-H. Cho, D. Mietchen, Y-S. Kim, K-S. Hong, C. Lee, D. Kang, K-D. Park, B-S. Choi, and C. Cheong. Subcellular In Vivo ^{1}H MR Spectroscopy of *Xenopus laevis* Oocytes. *Biophysical Journal*, 90(5):1797–1803, 2006. 12

[33] C. Juchem, T.W. Nixon, S. McIntyre, D.L. Rothman, and R.A. de Graaf. Magnetic field homogenization of the human prefrontal cortex with a set of localized electrical coils. *Magnetic Resonance in Medicine*, 63(1):171–180, 2010. 12

[34] P. Hudson, S.D. Hudson, W.B. Handler, and B.A. Chronik. Finite-Length Shim Coil Design Using a Fourier Series Minimum Inductance and Minimum Power Algorithm. *Concepts in Magnetic Resonance Part B (Magnetic Resonance Engineering)*, 37B:245–253, 2010. 12